

Published in final edited form as:

Stem Cell Res. 2012 January ; 8(1): 49–57. doi:10.1016/j.scr.2011.08.004.

Derivation of functional ventricular cardiomyocytes using endogenous promoter sequence from murine embryonic stem cells

Min Young Lee^{1,2}, Baonan Sun³, Simon Schliffke⁴, Zhichao Yue³, Mingyu Ye^{5,7}, Jere Paavola^{4,6}, Esra Cagavi Bozkulak^{1,2}, Peter J. Amos^{1,2}, Yongming Ren^{1,2}, Rong Ju¹, Yong Woo Jung⁸, Xin Ge, Lixia Yue³, Barbara E. Ehrlich⁴, and Yibing Qyang^{1,2,*}

¹Section of Cardiovascular Medicine, Department of Internal Medicine, Yale School of Medicine, New Haven, CT ²Yale Stem Cell Center, Yale School of Medicine, New Haven, CT ³Department of Cell Biology, Calhoun Cardiology Center, University of Connecticut Health Center, Farmington, CT ⁴Department of Pharmacology, Yale School of Medicine, New Haven, CT ⁵Department of Cellular and Molecular Physiology, Yale School of Medicine, New Haven, CT ⁶Minerva Foundation Institute for Medical Research, Biomedicum Helsinki 2U, Tukholmankatu 8, 00290, Helsinki, Finland ⁷Institute of Neuroscience, Chinese Academy of Sciences 320 Yue Yang Road, Shanghai 200031, China ⁸Department of Pharmaceutical Sciences, College of Pharmacy, Korea University, Korea

Abstract

The purpose of this study is to establish a murine embryonic stem cell (mESC) line for isolation of functional ventricular cardiomyocytes (VCMs) and then to characterize the derived VCMs. *By crossing the myosin light chain 2v (Mlc2v)-Cre mouse line with the reporter strain Rosa26-yellow fluorescent protein (YFP), We generated mESC lines from these double transgenic mice, in which Cre-mediated removal of a stop sequence results in the expression of YFP under the control of the ubiquitously active Rosa26 promoter specifically in the VCM.* After induction of differentiation via embryoid body (EB) formation, contracting YFP⁺ cells were detected within EBs and isolated by fluorescence-activated cell sorting. N-cadherin, the cadherin expressed in cardiomyocytes, and the major cardiac connexin (CX) isoform, CX43, were detected in the respective adherens and gap junctions in these VCMs. Using current clamp recordings we demonstrated that mESC-derived VCMs exhibited action potential characteristics comparable to those of neonatal mouse VCMs. Real-time intracellular calcium [Ca²⁺]_i imaging showed rhythmic intracellular calcium transients in these VCMs. The amplitude and frequency of calcium transients were increased by isoproterenol stimulation, suggesting the existence of functional β-adrenergic signaling. Moreover, [Ca²⁺]_i oscillations responded to increasing frequencies of external electrical stimulation, indicating that VCMs have functional excitation-contraction coupling, a key factor for the ultimate

© 2011 Elsevier B.V. All rights reserved.

*Correspondence to: Yibing Qyang PhD, Section of Cardiovascular Medicine, Yale Stem Cell Center, Yale School of Medicine, 300 George Street, Suite 773A, New Haven, CT 06520 FAX: 203-737-5528 Office: 203-737-6354 yibing.qyang@yale.edu.

Disclosures

None declared

Publisher's Disclaimer: This is a PDF file of an unedited manuscript that has been accepted for publication. As a service to our customers we are providing this early version of the manuscript. The manuscript will undergo copyediting, typesetting, and review of the resulting proof before it is published in its final citable form. Please note that during the production process errors may be discovered which could affect the content, and all legal disclaimers that apply to the journal pertain.

cardiac contractile performance. The present study makes possible the production of homogeneous and functional VCMs for basic research as well as for cardiac repair and regeneration.

Keywords

Embryonic stem cells; ventricular cardiomyocytes; cardiac differentiation

1. Introduction

Despite recent advances in pharmacological and surgical therapies, heart disease is the leading cause of mortality and morbidity worldwide [1]. Cardiac-related deaths due to ischemic heart disease are caused by occlusion of a coronary artery resulting in ventricular myocardial infarction (MI), which induces extensive myocardial cell death within the ischemic zone [2, 3], leading to heart failure [4]. Cell-based therapies are considered one of the most promising solutions to regenerate the damaged heart tissue. In the last decade, several groups reported that transplantation of isolated fetal or neonatal cardiomyocytes can aid in the regeneration of damaged heart tissue [5, 6]. *However, these studies were limited by the availability of fetal and neonatal cardiomyocytes*[7]. Current research seeks to address these issues by actively pursuing new strategies to derive novel/additional cell types useful for regenerative medicine from stem cells.

Embryonic stem cells (ESCs) are derived from the inner cell mass of the blastocyst stage embryos [8], and they have the ability to produce cells of all three germ layers, including heart cells [9]. Thus, they can provide an abundant, renewable source of cells for cardiac repair. Efforts have been made to develop strategies for cardiac lineage selection and cardiomyocyte differentiation using ESCs. Heterogenous cultures containing cardiac cells can be isolated from ESCs in culture [10–14]. Commonly, during cardiac differentiation in ESCs, all cardiac phenotypes including nodal, atrial and ventricular cells can be detected *in ESC cultures* [11, 15]. However, this phenotypic heterogeneity of differentiated ESC samples might lead to an inefficient engraftment and might cause abnormal electrical activity after implantation [16, 17]. Thus, it is critically important to isolate highly purified cardiac cells.

Ventricular cardiomyocytes (VCMs) are the most extensively injured cardiac cell type in ischemic heart disease and, as a result, the leading cause of reduced cardiac function. Therefore, it is of great interest to generate a renewable source of VCMs from ESCs for cell-based therapies to treat heart failure. Myosin light chain 2, ventricular isoform (*Mlc2v*) is specifically expressed in the ventricular chamber and is required for ventricular chamber morphogenesis during mammalian cardiogenesis [18, 19], providing an ideal marker for the isolation of VCMs. By using an artificial reporter system in which enhanced green fluorescent protein (*eGfp*) is driven by a hybrid promoter composed of a fragment of *Mlc2v* promoter and the enhancer element of the cytomegalovirus (CMV), two groups have previously established transgenic murine ESC (mESC) and embryonic carcinoma cell (ECC) lines for the isolation of VCMs, respectively [20, 21]. In the present study, we established a stable reporter system using endogenous promoter specifically activated in VCMs.

The *Mlc2v-Cre* mouse line, in which *Cre* is knocked into one of the endogenous *Mlc2v* loci, is a well-established strain for marking VCMs [18, 19]. By breeding this *Cre* line with the conditional *Cre* reporter strain *Rosa26*-yellow fluorescent protein (*Yfp*) [22], we generated ESC lines from the blastocysts of the double transgenic embryos (*Mlc2v-Cre; Rosa26-Yfp*) and isolated VCMs from these ESC lines by using *in vitro* differentiation. In this study, Cre-mediated removal of a stop sequence resulted in the expression of YFP under the control of

endogenous *Rosa26* promoter specifically in VCMs. We further showed that these ESC-derived VCMs displayed the capacity to form the functional syncytium, neonatal ventricular cardiomyocyte-like action potentials, and rhythmic intracellular calcium transients that are responsive to both chemical and electrical stimulation. This mESC line will allow the production of homogeneous, functional VCMs for cell-based ventricular repair and regeneration in murine heart injury models. This study will set the stage for the isolation of human VCMs using MLC2V as marker in human ESCs and induced pluripotent stem cells (iPSCs) for use in cardiac repair.

2. Results

2.1. Establishment of *Mlc2v-Cre; rosa26-Yfp* mESC line

We generated a mESC line using conditional genetic lineage tracing. *Mlc2v-Cre* mice were crossed into the conditional Cre reporter *Rosa26-YFP* strain. We isolated the *Mlc2v-Cre; Rosa26-Yfp* mESC line from day 3.5 embryos (Fig. 1A) and confirmed the presence of the *Mlc2v-Cre* and the *Yfp* genes in this mESC line by genomic DNA PCR analysis. Conversely, wild-type mice express neither *Mlc2v-Cre* nor the *Yfp* genes (Fig. 1B). Additionally, this *Mlc2v-Cre; Rosa26-Yfp* mESC line has a normal karyotype (Fig. 1C). To induce cardiac differentiation, embryoid bodies (EBs) derived from mESCs were cultured as previously described [23]. After 6 days following EB formation, scattered YFP expression was detectable in EBs. In order to examine whether YFP expression correlates with the presence of MLC2v proteins, mESC-derived beating cluster at day 10 was immunostained with anti-MLC2v antibody. This immunohistochemical data demonstrated the co-expression of YFP and MLC2v protein, which suggests the expression of VCM markers in YFP⁺ cells and YFP could be useful for the purification of VCMs. (Fig. 1D).

2.2. Characterization of FACS-sorted YFP⁺ VCMs

To characterize the cells expressing YFP in *Mlc2v-Cre; Rosa26-Yfp* cultures, EBs were enzymatically-dissociated into single cells at EB day 10 of cardiac differentiation for FACS analysis. Examination of the *Mlc2v-Cre; Rosa26-Yfp* mESC-derived EBs revealed a distinct population of YFP⁺ cells that were present in the *Mlc2v-Cre; Rosa26-Yfp* mESC-derived EBs, whereas no distinct YFP⁺ population was observed in EBs derived from wild type mESCs (Fig. 2A). To examine whether YFP⁺ cells were enriched for VCM marker *Mlc2v*, we analyzed FACS-sorted YFP⁺ cells with q-RT-PCR. Both *Mlc2v* and *Yfp* mRNA were highly enriched in YFP⁺ cells when compared to those in the YFP⁻ cell population (Fig. 2B). Additionally, immunocytochemical analysis revealed that FACS-sorted YFP⁺ cells were positive for the cardiomyocyte marker cardiac troponin T (cTnT). Taken together, our findings suggest that YFP⁺ cells have the characteristics of VCMs.

2.3. Formation of adherens and gap junctions in FACS-sorted YFP⁺ VCMs

We next examined the expression of cardiac junctional proteins in FACS-purified YFP⁺ VCMs. Immunofluorescence analysis showed that N-cadherin, a major isoform of cadherins in the adherens junction, and connexin 43, an important connexin isoform in the gap junctions of cardiomyocytes [24], were clearly expressed at cell-cell interfaces (Fig. 3A and 3B). These results suggest that YFP⁺ VCMs can form cardiac junctions. Importantly, *N-cadherin* and *Connexin 43* were also co-expressed with *MLC2v* in neonatal VCMs. Additionally, the protein expression levels and localization patterns for *N-cadherin* and *Connexin 43* were similar between neonatal VCMs and YFP⁺ VCMs (Fig. 3C and 3D). Our findings suggest that YFP⁺ VCMs express characteristic VCM junctional proteins and possess the ability to form cardiac junctions.

2.4. Action potential recordings of YFP⁺ VCMs

In order to examine the functionality of FACS-sorted YFP⁺ VCMs, cells were replated on gelatin-coated 25 mm glass coverslips (Fig. 4A), and we analyzed their action potential characteristics. Whole-cell current clamp electrophysiology analysis showed that FACS-purified YFP⁺ cells showed ventricular-like action potentials whereas atrial- or nodal-like action potentials were not observed (Fig. 4B). *The action potentials of YFP⁺ cells were comparable to those of neonatal mouse ventricular cardiomyocytes with respect to maximum diastolic potential (MDP) and upstroke velocity (dV/dt_{max}). Interestingly, we also observed that YFP⁺ VCMs showed a modest decrease in action potential amplitude (APA) and a significant prolongation of action potential duration at 90% repolarization (APD₉₀) as compared to neonatal mouse VCMs. These results suggest that our ES cell-derived VCMs exhibit action potentials characterized by premature ventricular patterns.*

2.5. [Ca²⁺]_i transient imaging of YFP⁺ VCMs

To determine the contractile properties of YFP⁺ VCMs, we performed real-time intracellular calcium [Ca²⁺]_i imaging analysis. After loading VCMs with the Ca²⁺ indicator dye, fluo-4 AM, we assessed changes in intracellular Ca²⁺ at a single-cell level in YFP⁺ cells by measuring minimum (Ca²⁺_{min}) and maximum (Ca²⁺_{max}) [Ca²⁺]_i using fluorescent microscopy (Fig 5A). Additionally, we observed periodic Ca²⁺ oscillations in YFP⁺ cells and found that both calcium transient amplitude and frequency were increased by isoproterenol treatment (Fig. 5B). Additionally, [Ca²⁺]_i oscillations responded to increasing frequencies of external electrical field stimulation (Fig. 5C). These data suggest that the β-adrenergic signaling pathway and cardiac *excitation-contraction coupling*, a key factor for the ultimate cardiac contractile performance, are present in YFP⁺ cells.

3. Discussion

MLC2v is expressed exclusively in the ventricles [18, 19], where it contributes to the formation of sarcomeres and increases Ca²⁺ sensitivity at submaximal Ca²⁺ concentrations [18, 26]. The present study demonstrates that *Mlc2v-Cre; Rosa26-Yfp* mESCs can differentiate into cardiac lineages and that VCMs can be isolated based on YFP expression. Several groups have reported that transplantation of cardiomyocytes derived from ESCs improves cardiac function after myocardial injury in rodent animal models [11, 27, 28]. However, successful therapy with ESC-derived donor cells is likely to require the generation of a highly purified cardiomyocyte population [27, 29]. Application of mixed cell populations into an injured left ventricle might trigger proarrhythmic effects due to the presence of inappropriate cell types such as nodal- and atrial-like cells [30]. In addition, a preparation containing undifferentiated cells could lead to tumorigenesis/teratoma formation. *Thus, the production of homogenous and functional cardiomyocytes is a prerequisite for cell based therapies.* To date, cardiomyocyte markers like alpha myosin heavy chain (α-MHC) [31] and α-actinin [32] have been used to isolate cardiomyocytes from ESCs. However, the cardiac differentiation of ESCs leads to a heterogeneous population of nodal-, atrial-, and ventricular-like derivatives [33, 34], and these markers lack the specificity needed for distinguishing between different types of cardiomyocytes. A significant percentage of cardiac-related deaths is due to ischemic heart disease related to myocardial infarction in the ventricles [35]. Therefore, it is critical to develop stem cell-based therapies for the regeneration of injured ventricular tissue.

We derived ESC lines from blastocysts of the double transgenic mouse line *Mlc2v-Cre; Rosa26-Yfp*, in which *Cre* and *Yfp* are specifically knocked into the *Mlc2v* and *Rosa26* gene loci, respectively. *Mlc2v-Cre-mediated removal of a stop sequence in the Rosa26-YFP reporter line results in expression of YFP under the control of the ubiquitous Rosa26*

promoter specifically in the VCM. Importantly, our analysis demonstrated that these YFP⁺ cells express both *Mlc2v* transcript and MLC2v protein compared to YFP⁻ cells by q-RT-PCR and immunocytochemistry. YFP⁺ cells were 1.05 ± 0.13 % and cTnT⁺ cells were 5.13 ± 0.01 % out of total cells in our system (Supplementary Fig. 1). This result suggests that approximately 20% of total cardiomyocytes are VCM (Supplementary Figure 1). It should be noted that YFP expression may not fully represent the total population of VCMs. Cre-mediated recombination and subsequent activation of YFP expression in VCMs is typically not 100%, which presents the possibility for the existence of VCMs that are not YFP⁺ (Fig. 1D). Furthermore, the ventricular identity and functionality of YFP⁺ cells were determined by analyzing electrophysiological characteristics. We observed that the action potentials (APs) of YFP⁺ cells showed ventricular morphology comparable to those of neonatal mouse ventricular cardiomyocytes, *as determined by maximum diastolic potential (MDP) and upstroke velocity (dV/dt_{max}).* Interestingly, we observed that YFP⁺ VCMs showed a modest decrease in action potential amplitude (APA) and a significant prolongation of action potential duration at 90% repolarization (APD₉₀) in comparison with neonatal mouse VCMs. Comparison of these electrophysiological values suggests that YFP⁺ cells isolated from EB day 10 are not as mature as neonatal ventricular cardiomyocytes [36]. In contrast to previous studies in which cardiomyocytes purified using promoter DNA constructs showed ventricular, atrial and nodal AP morphology, we observed exclusively ventricular AP morphology in our purified VCMs. We were also able to monitor Ca²⁺ transients, and we observed that our FACS-purified YFP⁺ cells showed periodic calcium oscillations that are responsive to both isoproterenol and electrical stimulation. Taken together, these results suggest that our FACS-purified YFP⁺ cells represent a differentiated ventricular cardiac phenotype.

Recently, two independent research groups utilized mitochondrial dyes and the cellular prion protein as markers to purify cardiomyocytes from ESCs without genetic manipulation [37, 38]. These represent an important step toward cardiomyocyte isolation without using genetic engineering methods. However, the cardiomyocytes isolated by these methods were still a mixture of atrial, ventricular and nodal cardiomyocytes. By using microarray analysis to compare the gene expression profiles of YFP⁺ VCMs and YFP⁻ cells derived from our current study, it may be possible to identify cell surface markers specific to VCMs and lead to the purification of VCMs with FACS, thereby avoiding the use of genetic engineering. In addition, VCMs hold the potential to be used as cell-based therapies for treatment of degenerative heart diseases.

Despite the advances presented in this work, several challenges remain. *Due to potential variations in the degree of cardiomyocyte differentiation between batches of differentiated ES cells, there may be non-uniformity when measuring action potentials and calcium transients of YFP⁺ VCMs. Therefore, techniques are needed to develop phenotypically mature cardiomyocytes, as opposed to the immature ventricular phenotype observed in this study.* Physiological stimuli such as mechanical stretch, shear stress and electrical pacing may help to promote cardiomyocyte maturation. Another challenge to be surmounted will be the development of a non-transgenic based approach to VCM isolation in order to maximize clinical application. Translation of the reported transgenic VCMs into clinical utility requires a non-transgenic approach to the isolation of VCMs. Future efforts are warranted to identify cell surface markers specific to VCMs using our purified transgenic VCMs. Third, in vivo electrical integration of VCMs with host cardiomyocytes needs to be investigated in the future in order to evaluate the potential of VCMs for cardiac repair.

4. Conclusion

This is the first study to derive functional VCMs using the *Mlc2v* endogenous promoter at a precise chromosomal locus. Our mESC line will allow the production of homogeneous and functional VCMs for basic research as well as for cell-based ventricular repair and regeneration. This strategy of using the human *MLC2v* endogenous promoter to direct the expression of a reporter construct can also be applied to human ES cells and induced pluripotent stem (iPS) cells for VCM isolation and cardiac research and cardiac repair.

5. Materials and Methods

5.1. Generation of *Mlc2v-Cre;Rosa26-Yfp* mouse embryonic stem cells (ESCs)

The *Mlc2v-Cre* mouse line, in which *Cre* was knocked into the endogenous *Mlc2v* locus, was crossed into the conditional *Cre* reporter strain *Rosa26-Yfp*, in which Cre-mediated removal of a stop sequence results in the ubiquitous expression of YFP under the control of an endogenous *Rosa26* promoter specifically in the ventricular cardiomyocytes. ESC lines were derived from these double transgenic mice as previously described [23]. Briefly, timed matings were performed and on embryonic day 3.5, the females were sacrificed and the blastocysts flushed from the uterine horns using M2 medium (Sigma-Aldrich, MO). After washing with M2 medium, the zona pellucid was removed with acidic Tyrode's Solution (Sigma-Aldrich, MO). After washing, the blastocysts were then adapted onto mouse embryonic feeder (MEF) cells for 7–10 days.

5.2. ESC culture and differentiation

Mouse ESCs were cultured for 3 days in Dulbecco's modified Eagle's medium (Invitrogen) supplemented with 1% penicillin and streptomycin (Invitrogen), 2 mM L-glutamine, 0.1 mM non-essential amino acid (MEM-NEAA; Invitrogen), 1mM sodium pyruvate (Invitrogen), 0.1 mM 2-mercaptoethanol (Sigma), LIF-conditioned media (1:500 dilution), and 15% Knock-out serum replacement (KO-SR; Invitrogen) on a mouse embryonic fibroblast (MEF) feeder layer. These cells were dissociated into single cells with 0.25% trypsin-EDTA (Invitrogen), and transferred to gelatin-coated 60 mm culture dishes and cultured in Iscove's modified Dulbecco's medium supplemented with 2mM L-glutamine, 1% penicillin and streptomycin, 0.1 mM 1-thioglycerol (Sigma), LIF-conditioned medium, and 15% KO-SR for 2 days, to deplete the feeder cells. For differentiation, 540 ESCs in 15 μ l aliquots of IMDM supplemented with 2mM L-glutamine, 0.1 mM 1-thioglycerol, and 15 % fetal bovine serum (FBS) were cultured in hanging drops for 2 days. The resultant individual embryoid bodies (EBs) were transferred to gelatin-coated culture dishes. Spontaneous contraction of EBs started 5.5 days after EB formation.

5.3. Fluorescence-activated cell sorting (FACS) and FACS analysis

At 10 days from EB formation, EBs were dissociated into single cell suspensions with a 1:1 solution of collagenase A and B (Roche) (6.67 mg/ml) for 30 min with periodic pipetting followed by digestion with Accutase[®] for 5 min. Cells were collected by centrifugation (1000 rpm for 5 min), washed with phosphate-buffered saline (PBS; Invitrogen), and then resuspended in PBS (1 ml) for FACS analysis. Sorting was performed using a Becton Dickinson FACSAria (BD Biosciences). YFP⁺ and YFP⁻ cells were sorted using the FL1 channel at low sheath pressure. Sorted cells were pelleted by centrifugation (1000 rpm for 5 min) and then used for subsequent applications. In addition, samples were also analyzed using FACSCalibur and Cell Quest software (BD Pharmingen).

5.4. Isolation of neonatal cardiomyocytes

Mouse hearts isolated from 1-day-old mouse pups were washed in ice-cold Hank's balanced salt solution without Ca^{2+} (HBSS) and predigested overnight in 0.5 mg/ml trypsin-HBSS solution at 4 °C under constant shaking. Cardiac cells were obtained after four rounds of 10 min digestions with 240 units/ml collagenase type II (Worthington) in HBSS at 37 °C. The cardiomyocyte fraction was separated from non-cardiomyocytes by two rounds of 1 hr differential plating on gelatin-coated culture dishes in DMEM/M-199 (3:1 ratio) medium containing 2 mM HBSS, 1% penicillin-streptomycin, 10% horse serum and 5% FBS at 37 °C. Under these condition non-cardiomyocytes preferentially attach on the culture dish. Non-adherent cardiomyocytes were collected and cultured until usage.

5.5. RNA isolation and quantitative RT-PCR

The total RNA was extracted using TRIzol[®] reagent and an RNA extraction kit (Qiagen). Reverse transcription was performed on a Mastercycler[®] system (Eppendorf) using an iScript cDNA synthesis Kit (Bio-rad). The real-time quantification of RNA targets was performed on a CFX96[™] real time system (Bio-Rad) using a Bio-Rad IQ SYBR green supermix (Bio-Rad). The primers were 5'-tgaccacacaagcagagagg-3' (sense), 5'-ccgtgggtaatgatgtggac-3' (antisense) for *Mlc2v*; 5'-ccctaccagcctacatgg-3' (sense), 5'-acatcgcagattgggtgtct-3' (antisense) for *Gata4*; 5'-catttaccgggagccctac-3' (sense), 5'-ctttgccagctcactgc-3' (antisense) for *Nkx2.5*; 5'-ggtgctgagtatgtcgtgga-3' (sense), 5'-cggagatgatgaccctttt-3' (antisense) for *Gapdh*. The reaction mixture (10 μ l) contained 100 ng of total RNA, 0.5 μ M of each primer, enzymes, and fluorescent dyes. The data was collected during the extension step and was analyzed using the manufacturer's software. The expression of genes of interest was normalized to that of *Gapdh* in qPCR.

5.6. Immunocytochemistry

YFP⁺ and YFP⁻ cells were plated in gelatin-coated culture plates and cultured for 3 days following FACS-sorting. Cells were fixed with 4% paraformaldehyde in PBS and permeabilized for 10 min with PBST (PBS containing 0.1% (v/v) Triton X-100) and washed 3 times with PBS, 10 min each wash. Cells were pre-incubated with 10% normal goat serum (NGS; Invitrogen) in PBST for 45 min in order to decrease non-specific antibody binding. Cells were then incubated for 60 min with primary antibody in a solution containing 1% (v/v) NGS in PBST and washed three times for 10 min with PBST. *Primary antibodies were as following: anti-Mlc2v antibody (1:20 dilution) (Alexis Corp., CA), anti-cTnT (1:500 dilution) (Lab Vision Corp., CA), anti-YFP antibody (1:400 dilution) (invitrogen), anti N-cadherin antibody (1:200 dilution) (Snata cruz biotechnology, CA), and anti connexin 43 antibody (1:200 dilution) (Sigma-aldrich, MO).* Cells were incubated with 1% (v/v) NGS for 60 min with FITC-conjugated anti-mouse or anti-rabbit secondary antibody (1:1000 dilution) (invitrogen) in PBST containing 1% (v/v) NGS, and washed three times with PBS, for 10 min each wash. Samples were visualized with a *confocal microscope (Nikon) and a fluorescence microscope (Nikon) with a 100 \times and 600 \times objectives.*

5.7. Whole-cell current clamp recording of action potentials

Action potential waveforms were recorded from single YFP⁺ cells or primary cultured mouse neonatal cardiomyocytes under whole-cell current clamp mode using an EPC9 patch-clamp amplifier and Pulse + Pulsefit software (HEKA Elektronik, Lambrecht/Pfalz, Germany) at room temperature. Patch pipettes were pulled from borosilicate glass tubes to give a resistance of 1.5 – 3.0 M Ω when filled with pipette solution. After formation of giga seal (> 1.5G Ω), whole-cell configuration was achieved by suction on the pipette in combination with Zap. The fast and slow capacity transients were canceled using computer-controlled circuitry of the patch-clamp amplifier before switching to current clamp mode.

Spontaneous action potential firings of the cells were recorded under continuous recording mode. Data were low-pass filtered at 2 kHz and digitized at a rate of 10 kHz. The bath solution contained 140 mM NaCl, 3 mM KCl, 1 mM CaCl₂, 1 mM MgCl₂, 10 mM HEPES, pH7.3 and the pipette solution was 145 mM KCl, 5 mM NaCl, 2 mM CaCl₂, 2 mM MgCl₂, 3 mM MgATP, 4 mM EGTA, 10 mM HEPES, pH7.3.

5.8. Calcium transient measurement

YFP⁺ cells were plated on gelatin-coated cover slips and cultured for 7 days. Cells were loaded with 25 μM cell permeant calcium indicator dye fluo-4 AM (Invitrogen) together with 0.1% Pluronic F-127 (Invitrogen) in Tyrode's solution containing 2.5 mM calcium at 37 °C for 30 min. Before imaging, the cells were allowed to de-esterify for 30 min in Tyrode's solution at 37°C. The coverslips were placed into a stimulation chamber (RC-21BRFS; Warner Instruments) containing Tyrode's solution and mounted onto an inverted fluorescence microscope (Nikon Diaphot-TDM). 30 μM blebbistatin (Sigma) was used in the chamber to arrest contraction of the cardiomyocytes. Measurements were repeated without blebbistatin to rule out its potential effect on the calcium transients. The sample was illuminated with a Nikon H-9 100W lamp powered by a short arc DC power supply (Chiu Technical Corporation) and the light was filtered with a Chroma 41001 filter set (HQ535/50m emission, HQ480/40x excitation, BS Q505LP dichroic; Chroma Technology Corporation). Data acquisition was performed at room temperature. Data was captured with a NeuroCCD camera (RedShirtImaging), acquired at 125 frames per second, and analyzed with Neuroplex Software (RedShirtImaging). Fluorescence was measured by manually defining each region of interest and quantified in relation to baseline fluorescence (F/F_0). The samples were electrically stimulated by field pacing (10v, 10 ms bipolar pulses at 1 - 4Hz). The samples were chemically stimulated with the β-adrenoceptor agonist isoproterenol (Sigma), which was added to the chamber and mixed for a final concentration of 500 nM.

5.9. Statistical analysis

The results were reported as the mean ± standard error of the mean (S.E.M.), and experiments were analyzed by Student's t-test. Statistical significance was defined as *P* values < 0.05.

Supplementary Material

Refer to Web version on PubMed Central for supplementary material.

Acknowledgments

This work was supported by the Yale cardiology startup fund [Y.Q.]; the American Heart Association [09SDG2080420 to Y.Q.]; National Institute of Health [1K02HL101990-01 and UL1 RR024139 to Y.Q.]; National Institute of Health [5T32 HL007950 to P.J.A.]; a grant from the Finnish Foundation for Cardiovascular Research [J.P.]; and National Institute of Health [DK57751 and DK061747 to B.E.E.]. We thank Dr. Lawrence Young for his critical review of this manuscript. We also thank Dr. Michael Simons for sharing with us his lab equipment and tissue culture space.

Abbreviations

The abbreviations used are

| | |
|------------|----------------------------|
| AP | action potential |
| APA | action potential amplitude |

| | |
|--------------|-----------------------------|
| APD | action potential duration |
| CMV | cytomegalovirus |
| MDP | maximum diastolic potential |
| cTnT | cardiac troponin T |
| EB | embryoid body |
| ECC | embryonic carcinoma cell |
| ESC | embryonic stem cell |
| GFP | green fluorescent protein |
| MEF | mouse embryonic fibroblast |
| MHC | myosin heavy chain |
| MI | myocardial infarction |
| MLC2v | myosin light chain 2v |
| VCM | ventricular cardiomyocyte |
| YFP | yellow fluorescent protein |

References

1. Jessup M, Brozena S. Heart failure. *N Engl J Med*. 2003; 348:2007–2018. [PubMed: 12748317]
2. Freude B, Masters TN, Robicsek F, et al. Apoptosis is initiated by myocardial ischemia and executed during reperfusion. *J Mol Cell Cardiol*. 2000; 32:197–208. [PubMed: 10722797]
3. Scarabelli T, Stephanou A, Rayment N, et al. Apoptosis of endothelial cells precedes myocyte cell apoptosis in ischemia/reperfusion injury. *Circulation*. 2001; 104:253–256. [PubMed: 11457740]
4. Gepstein L. Cell and gene therapy strategies for the treatment of postmyocardial infarction ventricular arrhythmias. *Ann N Y Acad Sci*. 2010; 1188:32–38. [PubMed: 20201883]
5. Müller-Ehmsen J, Peterson KL, et al. Rebuilding a damaged heart: long-term survival of transplanted neonatal rat cardiomyocytes after myocardial infarction and effect on cardiac function. *Circulation*. 2002; 105:1720–1726. [PubMed: 11940553]
6. Roell W, Lu ZJ, Bloch W, et al. Cellular cardiomyoplasty improves survival after myocardial injury. *Circulation*. 2002; 105:2435–2441. [PubMed: 12021233]
7. Reinecke H, Minami E, Zhu WZ, Laflamme MA. Cardiogenic differentiation and transdifferentiation of progenitor cells. *Circ Res*. 2008; 103:1058–1071. [PubMed: 18988903]
8. Evans MJ, Kaufman MH. Establishment in culture of pluripotential cells from mouse embryos. *Nature*. 1981; 292:154–156. [PubMed: 7242681]
9. Wobus AM, Kaomei G, Shan J, et al. Retinoic acid accelerates embryonic stem cell-derived cardiac differentiation and enhances development of ventricular cardiomyocytes. *J Mol Cell Cardiol*. 1997; 29:1525–1539. [PubMed: 9220339]
10. Kehat I, Kenyagin-Karsenti DM, et al. Human embryonic stem cells can differentiate into myocytes with structural and functional properties of cardiomyocytes. *J Clin Invest*. 2001; 108:407–414. [PubMed: 11489934]
11. Laflamme MA, Chen KY, Naumova AV, et al. Cardiomyocytes derived from human embryonic stem cells in pro-survival factors enhance function of infarcted rat hearts. *Nat Biotechnol*. 2007; 25:1015–1024. [PubMed: 17721512]
12. Maltsev VA, Wobus AM, Rohwedel J, Bader M, Hescheler J. Cardiomyocytes differentiated in vitro from embryonic stem cells developmentally express cardiac-specific genes and ionic currents. *Circ Res*. 1994; 75:233–244. [PubMed: 8033337]

13. Mummery C, Ward-van Oostwaard D, Eoendans P, et al. Differentiation of human embryonic stem cells to cardiomyocytes: role of coculture with visceral endoderm-like cells. *Circulation*. 2003; 107:2733–2740. [PubMed: 12742992]
14. Xu C, Police S, Rao N, Carpenter MK. Characterization and enrichment of cardiomyocytes derived from human embryonic stem cells. *Circ Res*. 2002; 91:501–508. [PubMed: 12242268]
15. Yang L, Soonpaa MH, Adler ED, et al. Human cardiovascular progenitor cells develop from a KDR⁺ embryonic-stem-cell-derived population. *Nature*. 2008; 453:524–528. [PubMed: 18432194]
16. Zhu WZ, Xie Y, Moyes KW, Gold JD, Askari B, Laflamme MA. Neuregulin/ErbB signaling regulates cardiac subtype specification in differentiating human embryonic stem cells. *Circ Res*. 2010; 107:776–786. [PubMed: 20671236]
17. Hansson EM, Lindsay ME, Chien KR. Regeneration next: toward heart stem cell therapeutics. *Cell Stem Cell*. 2009; 5:364–377. [PubMed: 19796617]
18. Chen J, Kubalak SW, Price S, et al. Selective requirement of myosin light chain 2v in embryonic heart function. *J Biol Chem*. 1998; 273:1252–1256. [PubMed: 9422794]
19. Minamisawa S, Gu Y, Ross J Jr, Chien KR, Chen J. Post-transcriptional compensatory pathway in heterozygous ventricular myosin light chain 2-deficient mice results in lack of gene dosage effect during normal cardiac growth or hypertrophy. *J Biol Chem*. 1999; 274:10066–10070. [PubMed: 10187786]
20. Moore JC, Spijker R, Martens AC, et al. A P19Cl6 GFP reporter line to quantify cardiomyocyte differentiation of stem cells. *Int J Dev Biol*. 2004; 48:47–55. [PubMed: 15005574]
21. Müller M, Fleischmann BK, Selbert S, et al. Selection of ventricular-like cardiomyocytes from ES cells in vitro. *FASEB J*. 2000; 14:2540–2548. [PubMed: 11099473]
22. Abou-Khalil R, Le Grand F, Pallafacchina G, et al. Autocrine and paracrine angiopoietin 1/Tie-2 signaling promotes muscle satellite cell self-renewal. *Cell Stem Cell*. 2009; 5:298–309. [PubMed: 19733541]
23. Qyang Y, Martin-Puig S, Chiravuri M, et al. The renewal and differentiation of Isl1+ cardiovascular progenitors are controlled by a Wnt/beta-catenin pathway. *Cell Stem Cell*. 2007; 1:165–179. [PubMed: 18371348]
24. Noorman M, van der Heyden MA, van Veen TA, et al. Cardiac cell-cell junctions in health and disease: Electrical versus mechanical coupling. *J Mol Cell Cardiol*. 2009; 47:23–31. [PubMed: 19344726]
25. Yu D, Buibas M, Chow SK, et al. Characterization of Calcium-Mediated Intracellular and Intercellular Signaling in the rMC-1 Glial Cell Line. *Cell Mol Bioeng*. 2009; 2:144–155. [PubMed: 19890481]
26. Olsson MC, Patel JR, Fitzsimons DP, Walker JW, Moss RL. Basal myosin light chain phosphorylation is a determinant of Ca²⁺ sensitivity of force and activation dependence of the kinetics of myocardial force development. *Am J Physiol Heart Circ Physiol*. 2004; 287:H2712–H2718. [PubMed: 15331360]
27. Klug MG, Soonpaa MH, Koh GY, Field LJ. Genetically selected cardiomyocytes from differentiating embryonic stem cells form stable intracardiac grafts. *J Clin Invest*. 1996; 98:216–224. [PubMed: 8690796]
28. van Laake LW, Passier R, Monshouwer-Kloots J, et al. Human embryonic stem cell-derived cardiomyocytes survive and mature in the mouse heart and transiently improve function after myocardial infarction. *Stem Cell Res*. 2007; 1:9–24. [PubMed: 19383383]
29. Zandstra PW, Bauwens C, Yin T, et al. Scalable production of embryonic stem cell-derived cardiomyocytes. *Tissue Eng*. 2003; 9:767–778. [PubMed: 13678453]
30. Zhang J, Wilson GF, Soerens AG, et al. Functional cardiomyocytes derived from human induced pluripotent stem cells. *Circ Res*. 2009; 104:e30–e41. [PubMed: 19213953]
31. Kita-Matsuo H, Barcova M, Prigozhina N, et al. Lentiviral vectors and protocols for creation of stable hESC lines for fluorescent tracking and drug resistance selection of cardiomyocytes. *PLoS One*. 2009; 4:e5046. [PubMed: 19352491]
32. Kolossov E, Fleischmann BK, Liu Q. Functional characteristics of ES cell-derived cardiac precursor cells identified by tissue-specific expression of the green fluorescent protein. *J Cell Biol*. 1998; 143:2045–2056. [PubMed: 9864374]

33. He JQ, Ma Y, Lee Y, Thomson JA, Kamp TJ. Human embryonic stem cells develop into multiple types of cardiac myocytes: action potential characterization. *Circ Res*. 2003; 93:32–39. [PubMed: 12791707]
34. Moore JC, Fu J, Chan YC, et al. Distinct cardiogenic preferences of two human embryonic stem cell (hESC) lines are imprinted in their proteomes in the pluripotent state. *Biochem Biophys Res Commun*. 2008; 372:553–558. [PubMed: 18503758]
35. Thom T, Haase N, Rosamond W, et al. Heart disease and stroke statistics--2006 update: a report from the American Heart Association Statistics Committee and Stroke Statistics Subcommittee. *Circulation*. 2006; 113:e85–e151. [PubMed: 16407573]
36. Wang LJ, Sobie EA. Mathematical model of the neonatal mouse ventricular action potential. *Am J Physiol Heart Circ Physiol*. 2008; 294:H2565–H2575. [PubMed: 18408122]
37. Hattori F, Chen H, Yamashita H, et al. Nongenetic method for purifying stem cell-derived cardiomyocytes. *Nat Methods*. 2010; 7:61–66. [PubMed: 19946277]
38. Hidaka K, Shirai M, Lee JK, et al. The cellular prion protein identifies bipotential cardiomyogenic progenitors. *Circ Res*. 2010; 106:111–119. [PubMed: 19910576]

Research highlights

A mixed population of cardiomyocytes can be isolated from embryonic stem cells (ESCs). However, they may cause abnormal electrical activity after implantation. We developed a ventricular cardiomyocytes (VCMs) purification system from mouse ESCs. We used the endogenous myosin light chain 2v (*Mlc2v*) promoter which is VCM specific. These VCMs have typical electrophysiological function. They may be effective for cardiac regenerative therapy.

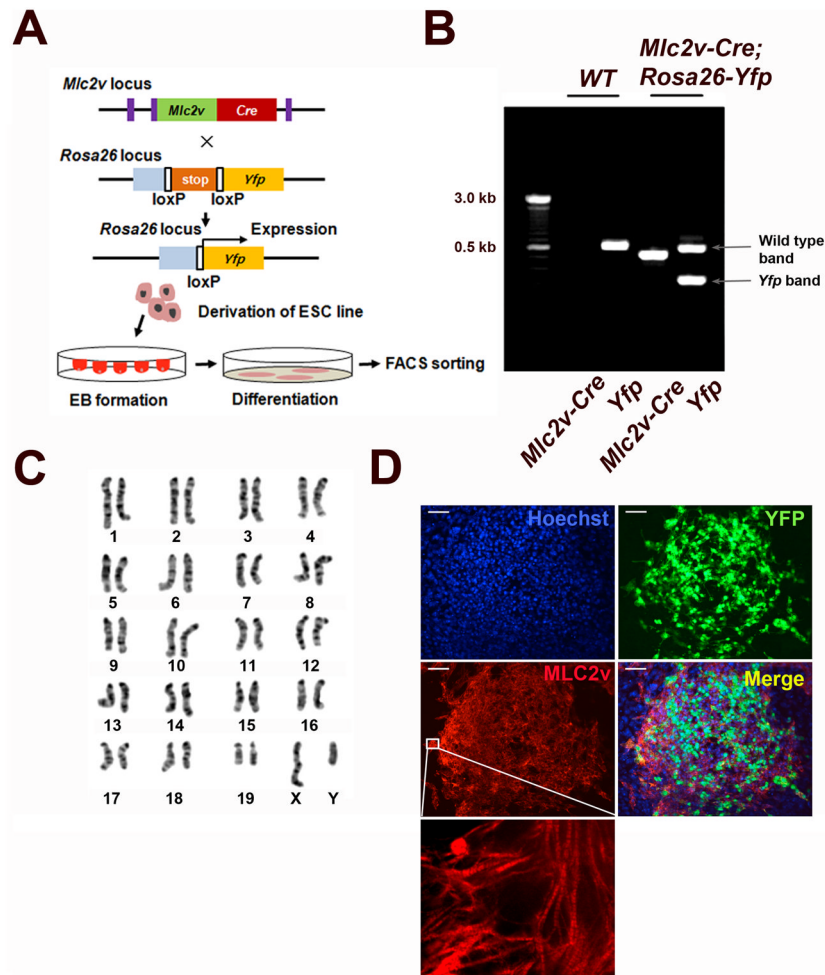


Figure 1.

Derivation of mESC line for isolation of VCMs. (A) A Schematic diagram of derivation of the *Mlc2v-Cre; Rosa26-Yfp* double transgenic mESC line and the isolation of VCMs. Mice carry one *Mlc2v-Cre* allele and one *Rosa26-Yfp* reporter gene. (B) PCR-based genotyping of the *Mlc2v-Cre* and *Yfp* genes in the *Mlc2v-Cre; Rosa26-Yfp* double transgenic mESC line and wild type control (WT). (C) G-banding chromosome analysis of the *Mlc2v-Cre; Rosa26-Yfp* mESC line. (D) Immunocytochemical characterization of mESC-derived ventricular cardiomyocytes. Day 10 EBs were dissociated and replated on the culture plate. YFP fluorescent cells express MLC2v protein in beating clusters. Inset represents magnified views of the white boxes which shows striation pattern of MLC2v. Scale bar, 100 μ m.

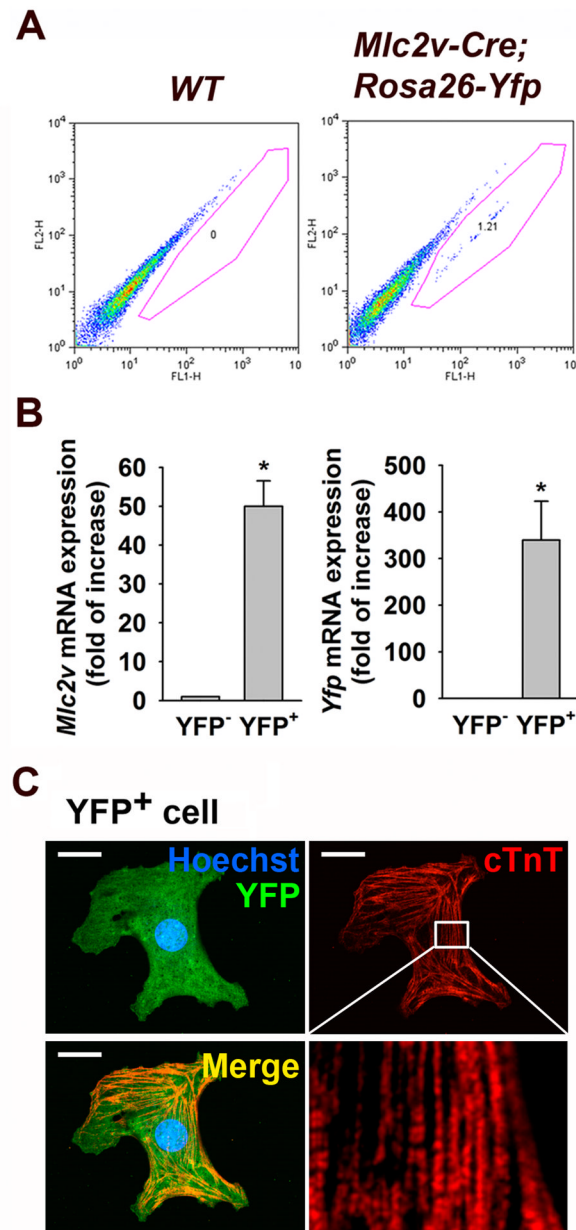


Figure 2. Isolation of *Mlc2v-Cre;Rosa26-Yfp* mESC-derived VCMs. (A) Flow cytometry profile of EB day 10 differentiated *Mlc2v-Cre;Rosa26-Yfp* mESC-derived VCMs. Wild type mESCs were used as a negative control. (B) Quantitative PCR (qPCR) analysis showing *Mlc2v* and *Yfp* gene expression in YFP⁻ cells compared to YFP⁺ cells isolated from day 10 *Mlc2v-Cre;Rosa26-Yfp* EBs. The values are reported as the mean \pm S.E.M.. (n = 3). * $P < 0.05$ vs. YFP⁻. (C) Immunostaining of FACS-sorted YFP⁺ cell from day 10 *Mlc2v-Cre;Rosa26-Yfp* EBs shows cTnT expression. Inset represents magnified views of the white boxes which shows striation pattern of cTnT. Scale bar, 20 μ m.

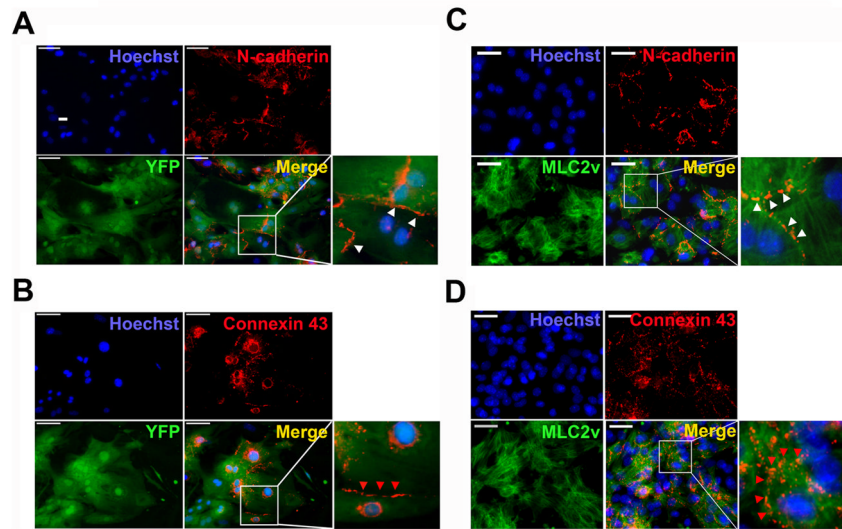


Figure 3. N-cadherin and Cx43 protein expression in YFP⁺ VCMs and neonatal VCMs. Immunocytochemistry showed that N-cadherin and Cx43 are expressed in FACS-sorted YFP⁺ VCMs (A and B) and *MLC2v* expressing neonatal VCMs (C and D). Insets represent magnified views of the white boxes and show that N-cadherin (white arrow heads) and Cx43 (red arrow heads) are expressed at cell-cell interface. Scale bar, 50 μ m.

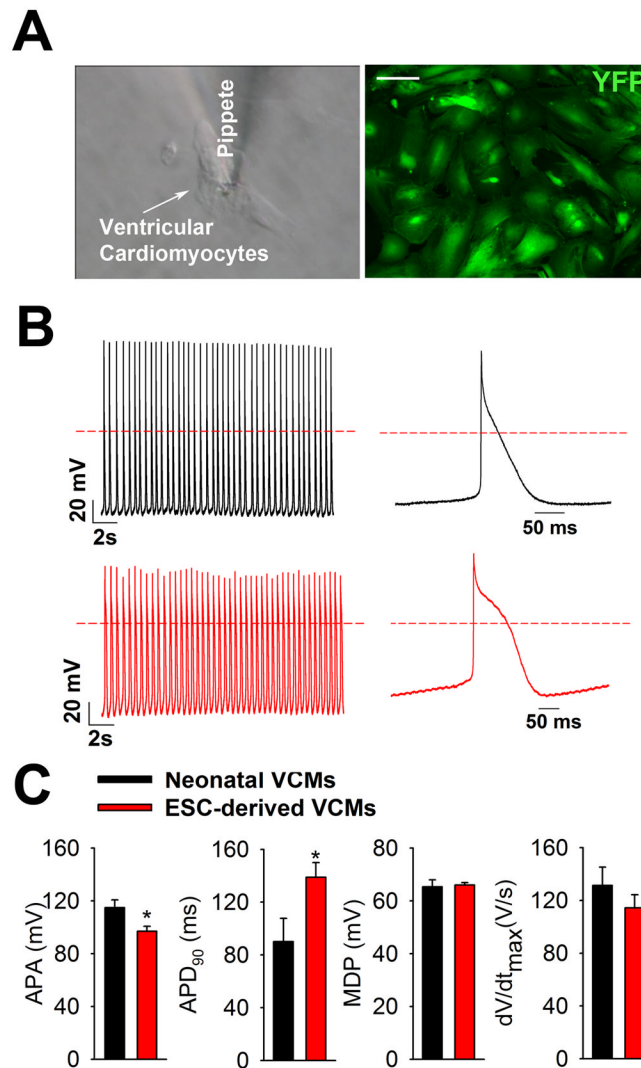


Figure 4. Action potential recording in contracting FACS-sorted YFP⁺ VCMs. (A) Representative image of FACS-sorted YFP⁺ VCMs in which action potentials are recorded by whole-cell current clamp mode using a patch-clamp amplifier. Scale bar, 100 μ m. (B) Action potentials in a YFP⁺ VCMs and a neonatal VCMs. (C) Summarized data showing dV/dt (the maximum rate of rise of action potential stroke), APA (action potential amplitude), APD₉₀ (action potential duration at 90% of repolarization) and MDP (the maximum diastolic potential). Neonatal VCMs ($n=20$) and YFP⁺ VCMs ($n=40$) from 3 different batches were analyzed. The values are reported as the mean \pm S.E.M.

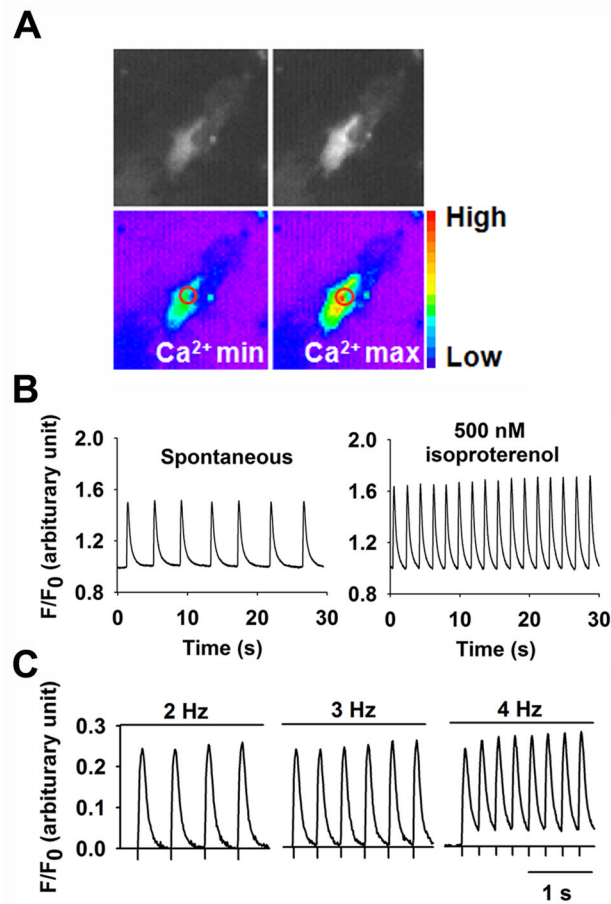


Figure 5.

Real time $[Ca^{2+}]_i$ transients in contracting FACS-sorted YFP⁺ VCMs. (A) Representative fluorescence and pseudo-colored images of spontaneous contracting YFP⁺ VCMs showing minimal (Ca^{2+}_{min}) and maximal (Ca^{2+}_{max}) fluo-4 fluorescence intensity. Circles indicate the area used to measure Ca^{2+} . (B) Increase in $[Ca^{2+}]_i$ transient amplitude and frequency in YFP⁺ VCMs under isoproterenol stimulation (500 nM). (C) Calcium transients of YFP⁺ VCMs in response to electrical pacing at various frequencies.